

Molecular Cell, Volume 70

Supplemental Information

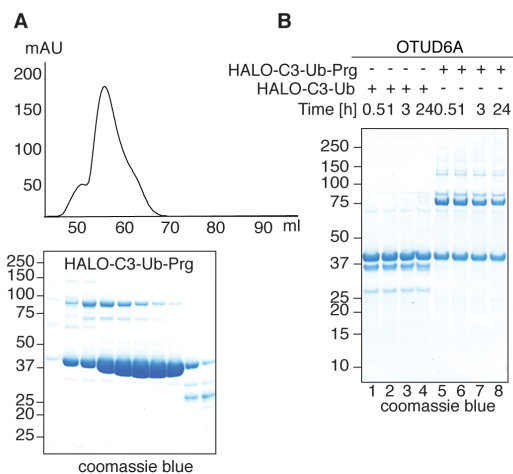
Discovery and Characterization

of ZUFSP/ZUP1, a Distinct Deubiquitinase

Class Important for Genome Stability

Dominika Kwasna, Syed Arif Abdul Rehman, Jayaprakash Natarajan, Stephen Matthews, Ross Madden, Virginia De Cesare, Simone Weidlich, Satpal Virdee, Ivan Ahel, Ian Gibbs-Seymour, and Yogesh Kulathu

Supplementary Figure Legends



D

SEQUENCE	INTENSITY HEK293 HALO-C3-UB-PRG	START POSITION	END POSITION
MLSCNICGETVTSEPD M K	1268600	1	18
HEGFYSENLTESR	1444800	115	127
GSVYETTYSPPECPFCGK	2055500	144	161
QEIEEFQK	2527400	255	262
EGFDPPQASQLN N R	1716200	403	416

SEQUENCE	INTENSITY JURKAT HALO-C3-UB-PRG	START POSITION	END POSITION
MLSCNICGETVTSEPD M K	238550	1	18
INTVQYGTSDNK	918930	65	76
DNTLQCGMEVNSSILSGCASNHPK	5510200	78	101
GSVYETTYSPPECPFCGK	1817500	144	161
IEHSEDMETHVK	9126500	162	174
VQCSGDLQLAHLQEQEEDR	3988200	228	246
QYGLD N SGGYK	2433400	266	276
EGFDPPQASQLN N R	1474700	403	416

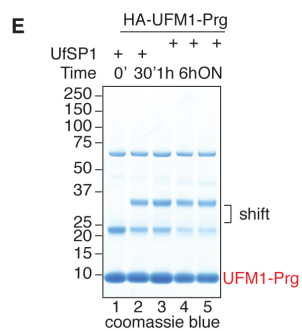


Figure S1

C

NR	DUB	Mass	JURKAT	HEK293	DUB FAMILY
1	USP9X	292 kDa	+	+	USP
2	USP24	294 kDa	+	+	
3	USP7	128 kDa	+	+	
4	USP47	157 kDa	+	+	
5	USP11	110 kDa	+	+	
6	USP5	96 kDa	+	+	
7	USP19	146 kDa	+	+	
8	USP14	56 kDa	+	+	
9	USP25	122 kDa	+	+	
10	USP32	182 kDa	+	+	
11	USP8	128 kDa	+	+	
12	USP4	109 kDa	+	+	
13	UBP48	119 kDa	+	+	
14	UBP34	404 kDa	+	+	
15	UBP15	112 kDa	+	+	
16	UBP13	97 kDa	+	+	
17	UBP10	87 kDa	+	+	
18	UBP28	122 kDa	+	+	
19	UBP37	110 kDa	+	+	
20	UBP38	117 kDa	+	+	
21	UBP16	94 kDa	+	+	
22	CYLD	107 kDa	+	+	
23	UBP20	102 kDa	+	+	
24	UBP42	145 kDa	+	+	
25	UBP40	140 kDa	+	+	
26	UBP3	59 kDa	+	+	
27	UBP33	107 kDa	+	+	
28	UBP22	60 kDa	+	+	
29	UBP30	59 kDa	+	+	
30	UBP45	92 kDa	+	+	
31	UBP35	113 kDa	+	+	
32	UBP6	159 kDa	+	+	
33	UBP36	123 kDa	+	+	
34	UBP27	50 kDa	+	+	
35	UBP53	121 kDa	-	+	
36	UBP31	147 kDa	-	+	
37	UBP54	187 kDa	-	+	
38	UBP2	68 kDa	-	+	
39	UBP46	42 kDa	-	+	
40	VCIPI1	134 kDa	+	+	OTU
41	OTUD4	124 kDa	+	+	
42	OTU7B	93 kDa	+	+	
43	OTUD5	61 kDa	+	+	
44	OTU1	38 kDa	+	+	
45	OTU6B	34 kDa	+	+	
46	OTUD3	45 kDa	+	+	
47	OTUB2	27 kDa	+	+	
48	OTU7A	101 kDa	+	+	
49	OTUD1	51 kDa	+	+	
50	OTULIN	40 kDa	+	-	UCHL
51	OTUB1	31 kDa	-	+	
52	UCHL5	38 kDa	+	+	
53	BAP1	80 kDa	+	+	
54	UCHL3	26 kDa	+	+	MINDY
55	UCHL1	25 kDa	-	+	
56	FAM63B	67 kDa	+	+	
57	FAM188A	50 kDa	+	+	MJD
58	FAM188B	84 kDa	+	+	
59	FAM63A	52 kDa	-	+	
60	ATX3	42 kDa	+	+	?
61	JOSD1	23 kDa	+	+	
62	AT7L3	39 kDa	+	+	
63	JOSD2	21 kDa	+	+	
64	ZUFSP	66 kDa	+	+	

Figure S1 (related to Figure 1).

Activity based protein profiling of DUBs identifies ZUFSP as a putative DUB

(A) Protein profile and Coomassie Blue stained gel of HALO-C3-Ub-Prg probe after purification by size exclusion chromatography.

(B) Analysis of probe activity by incubating HALO-C3-Ub-Prg and HALO-C3-Ub with the well characterised DUB OTUD6A. Samples were separated by SDS-PAGE gel and visualised by Coomassie Blue staining.

(C) Full list of the annotated DUBs discovered by mass spectrometry analysis from the Ub-Prg probe after incubation with HEK293 and JURKAT cells. DUB family names are shown in the last column.

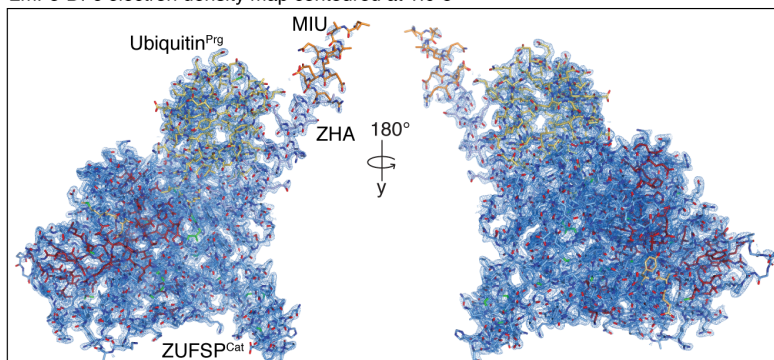
(D) Details of ZUFSP peptides identified by mass spectrometry analysis following Ub-Prg probe pull downs from HEK293 or JURKAT cell extracts.

(E) Reaction of HA-UFM1-Prg probe with UfSP1 (Mm). Samples were separated by SDS-PAGE gel and visualised by Coomassie Blue staining.

Figure S2

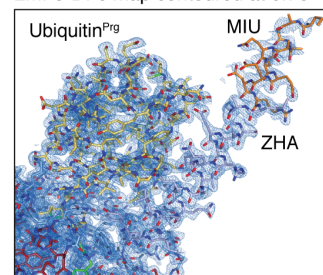
A

2mFo-DFc electron density map contoured at 1.0 σ



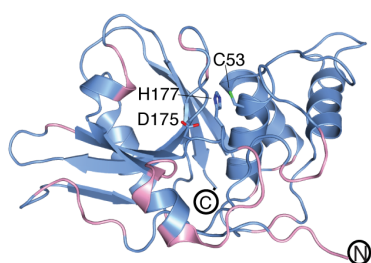
B

2mFo-DFc map contoured at 0.7 σ



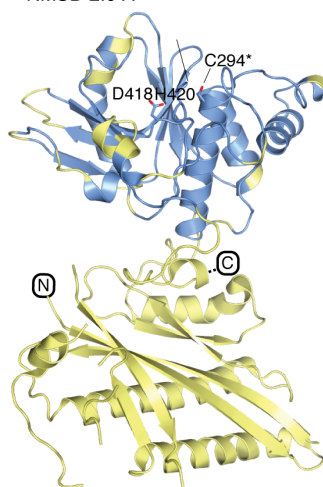
C

UfSP1 (PDB code 2Z84)
RMSD 2.35 Å



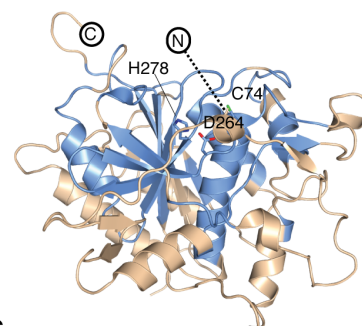
D

UfSP2 (PDB code 3OQC)
RMSD 2.0 Å



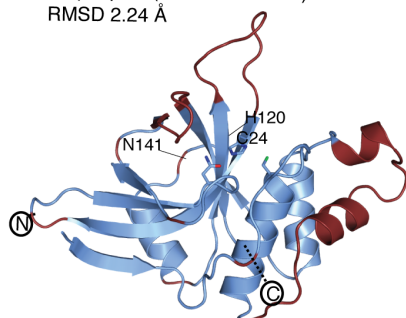
E

ATG4B (PDB code 2D11)
RMSD 2.3 Å

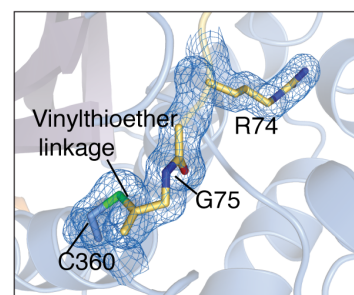


F

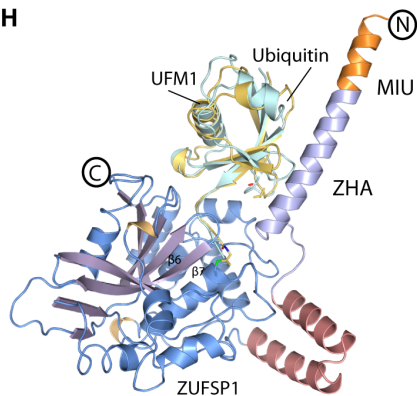
Staphopain (PDB code 1CV8)
RMSD 2.24 Å



G



H



I

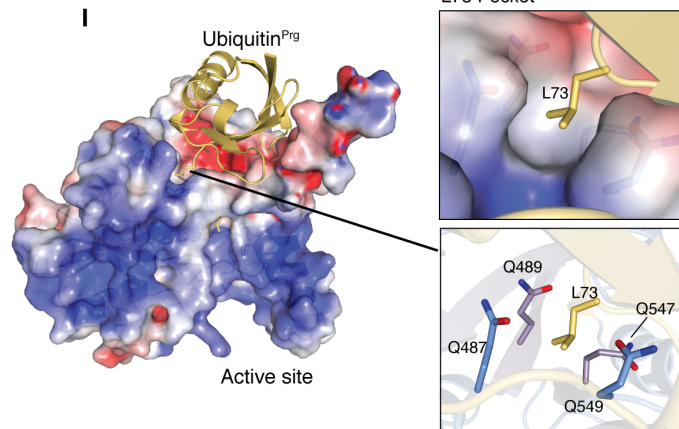


Figure S2 (related to Figure 2).

Crystal structure of ZUFSP in complex with distal ubiquitin

(A) $2|F_o| - |F_c|$ electron density map of the asymmetric unit for the ZUFSP~Ub-Prg complex contoured at 1σ .

(B) $2|F_o| - |F_c|$ electron density map of the ZHA-MIU region contoured at 0.7σ . The electron density for the residues from 236 till 239 is poor and the residues in this range have been built at 50% occupancy.

(C-F) Superposition of ZUFSP with UFSP1, UFSP2, ATG4B and Staphopain. The aligned regions of these structures are depicted in blue. The structural alignment was done in coot using Secondary Structure Matching (SSM) superposition method.

(G) Weighted $2|F_o| - |F_c|$ electron density map of catalytic cysteine in covalent linkage with ubiquitin-Prg contoured at 1σ .

(H) Structural superposition of UFM1 onto the ZUFSP-Ub-Prg complex structure. Ubiquitin and UFM1 are coloured in yelloworange and lightcyan, respectively.

(I) Close up view of the L73 pocket formed by the aliphatic side chains of glutamine residues is shown both in surface representation and sticks. Negative electrostatic surface is shown in red and positive surface in blue and hydrophobic in white. The surfaces are drawn at $\pm 4e/kBT$

Figure S3

A

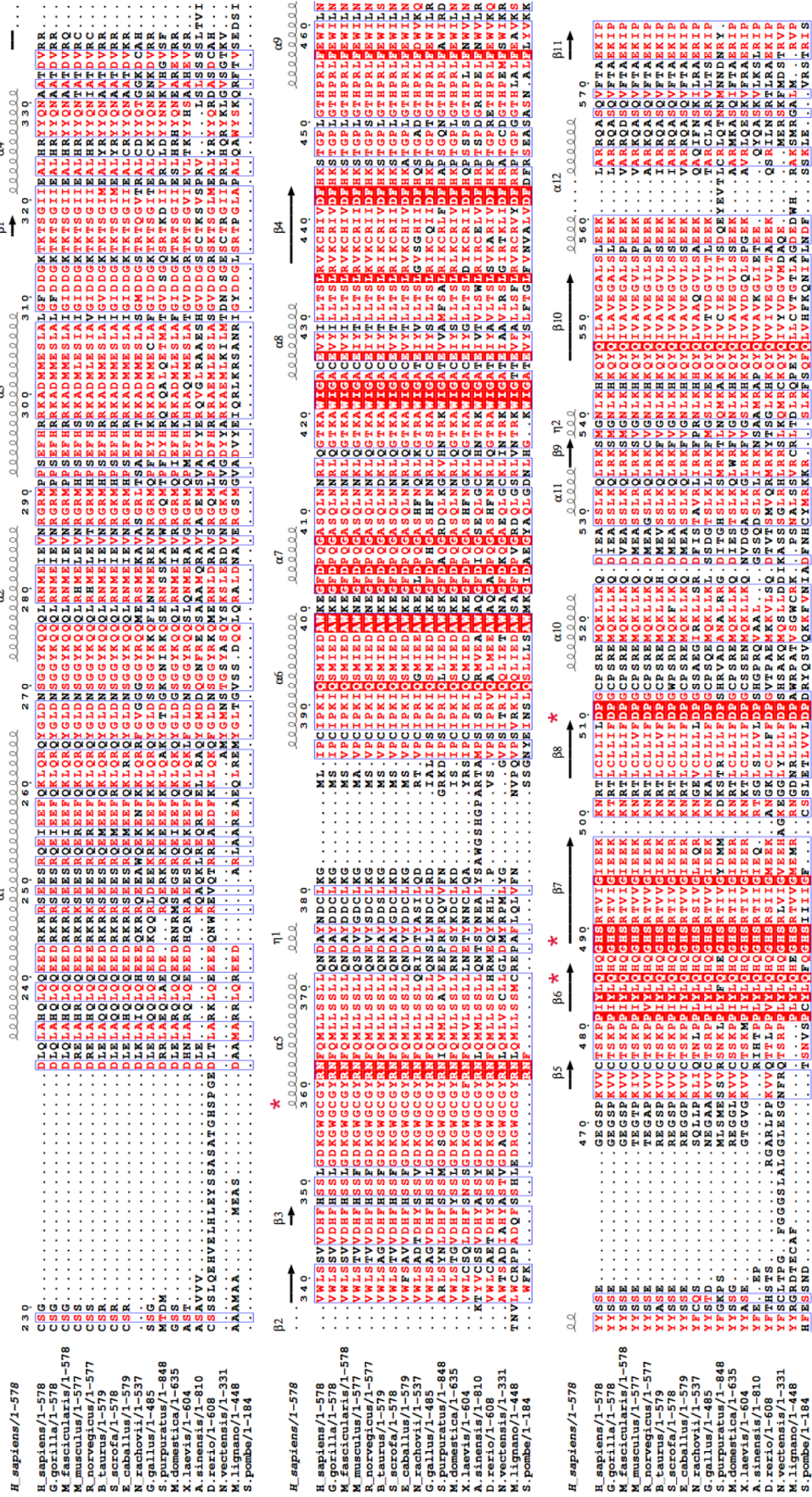


Figure S3 (related to Figure 2,3).

ZUFSP is evolutionary conserved.

Sequence alignment of the catalytic domain of ZUFSP from different species (human, gorilla, monkey, mouse, rat, bovine, pig, horse, fish, chicken, sea urchin, fly, frog, alligator, zebrafish, sea anemone, flatworm, yeast). The region covering the catalytic domain shows relatively higher degree of evolutionary conservation. Fully conserved residues are shaded in red. Secondary structure elements are represented by coil and arrows for alpha helix and beta sheets respectively. The catalytic residues are highlighted in red asterisks.

Figure S4

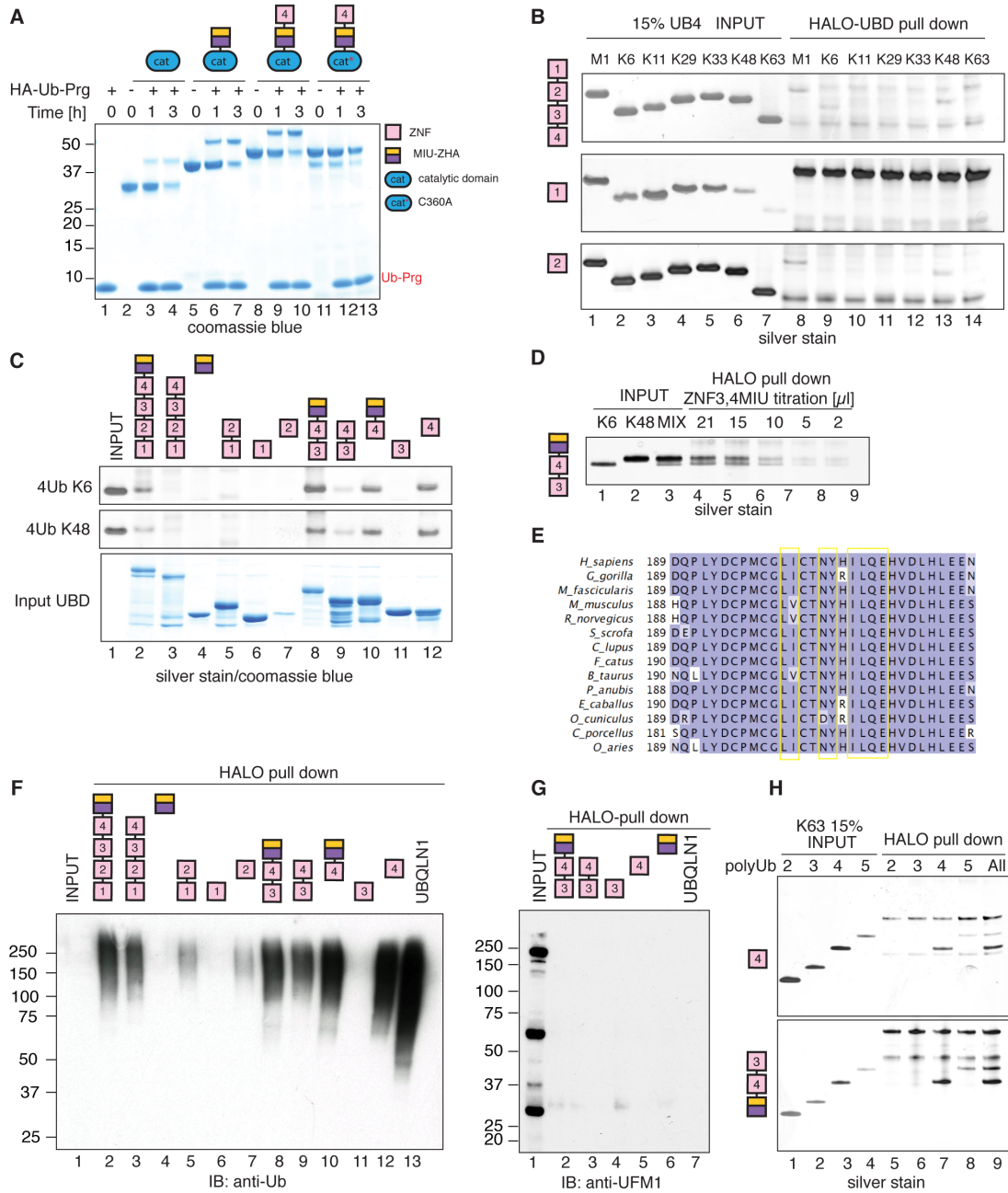


Figure S4 (related to Figure 3).

Characterization of ubiquitin binding domains in ZUFSP

(A) The indicated recombinant ZUFSP proteins were incubated with the HA-Ub-Prg probe. Reactions were separated by SDS-PAGE and visualised by Coomassie Blue staining.

(B) HALO-tag proteins were immobilised on HALO Link resin and incubated with tetra-Ub of different linkages. Bound material was separated by SDS-PAGE and silver stained.

(C) Comparison of polyUb binding by different domains of ZUFSP. Bound material was analysed as in (B). In the bottom panel, 5 % of input UBD stained by Coomassie Blue is shown.

(D) Competitive binding assay of K6 and K48 4Ub by HALO-ZUFSP ZNF3,4MIU (145-267). Bound material was analysed as in (B).

(E) Multiple sequence alignment of ZNF4 (189-219) of ZUFSP from different species. Yellow boxes highlight residues mutated, and tested for binding ability, shown in **Figure 4F**.

(F-G) PolyUb chains isolated from mammalian cells with recombinant domains of ZUFSP. HEK293 cell lysate was incubated with the indicated domains immobilised to HALO-tag resin. Bound material was visualised by anti-Ub and anti-UFM1 immunoblotting.

(H) The indicated ZUFSP HALO-Tag fusion proteins were coupled to HALO Link beads and incubated with di-, tri-, tetra-, or penta-K63Ub. The last well shows competitive pull down with di-, tri-, tetra- and penta-Ub mixed together. Bound material was analysed as in (B).

Figure S5

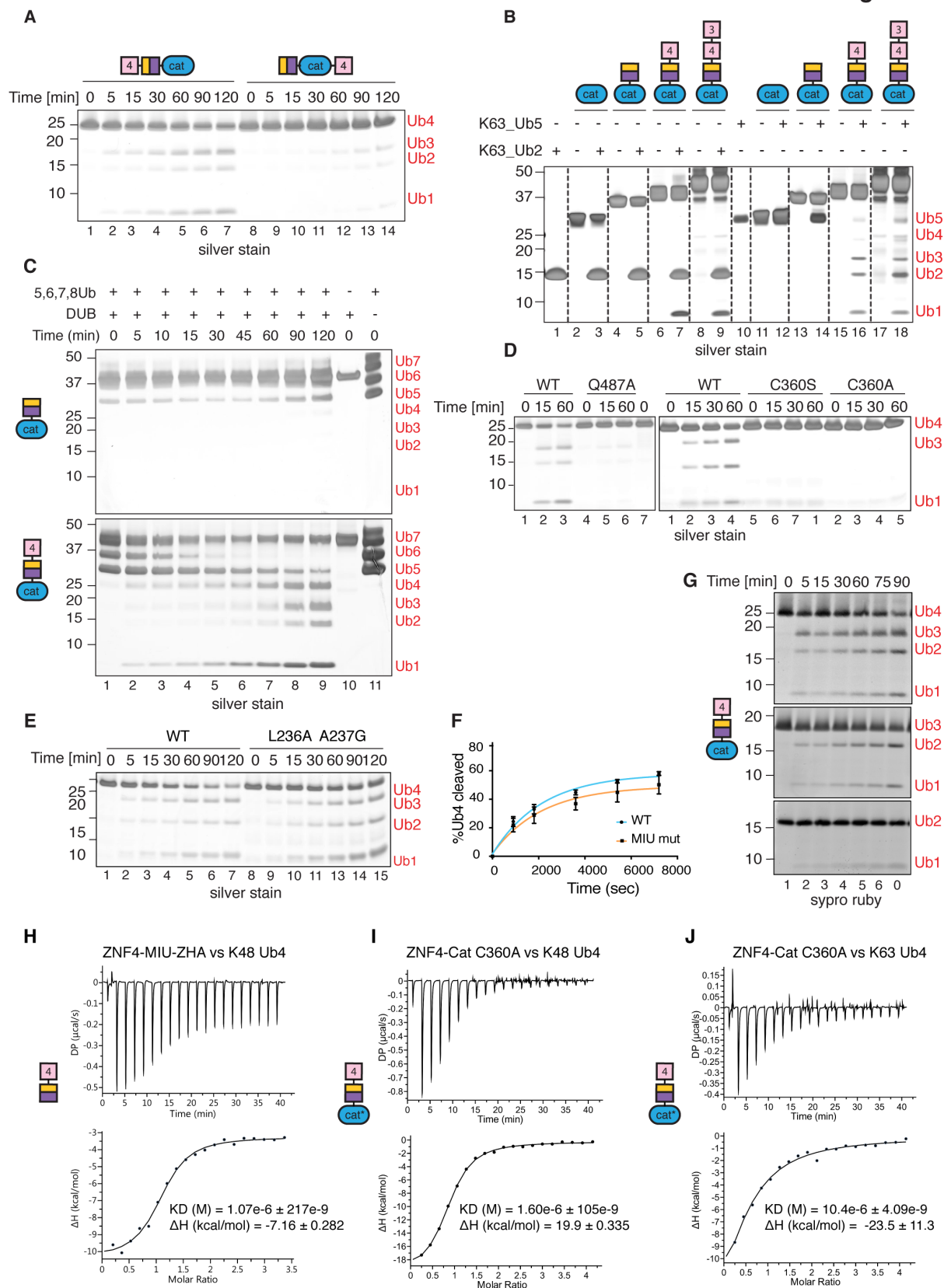


Figure S5 (related to Figure 5).

Analysis of DUB activity of ZUFSP

(A) Deubiquitinase assay monitoring activity of ZUFSP^{ZNF4-MIU-Cat} and ZUFSP^{MIU-Cat-ZNF4}. The enzymes were incubated with K63-tetraUb for the indicated times. Reaction products were separated by SDS-PAGE and visualized by silver staining.

(B) Cleavage of K63-linked pentaUb chains by the indicated ZUFSP constructs. Reaction products were visualized by silver staining.

(C) Activity of ZUFSP towards long K63-linked chains was analyzed in a time course monitoring cleavage of mixed penta-, hexa- and hepta-K63-linked poly-Ub chains by ZUFSP^{MIU-Cat} or ZUFSP^{ZNF4-MIU-Cat}. Reaction products were visualised by silver staining.

(D) Analysis of Q487A mutation on DUB activity and comparison of mutation of catalytic cysteine to serine or alanine. Reaction products were visualized by silver staining.

(E) Comparison of ZUFSP^{ZNF4MIU-Cat} WT with double point mutant in the MIU motif (L263A, A237G). Time course examining cleavage of K63-linked tetraUb. Reaction products were separated by SDS-PAGE and visualized by silver staining.

(F) Time course comparing activity of ZUFSP^{ZNF4-MIU-Cat} WT and the MIU mutant (L263A, A237G). Percentage of cleaved tetra-ubiquitin was quantified from Sypro Ruby-stained gels. Data from three independent experiments were fitted using nonlinear regression, one phase exponential decay. SD error bars are shown.

(G) Time course comparing cleavage of K63 chains of different lengths by ZUFSP^{ZNF4-MIU-Cat}. Reaction products were separated by SDS-PAGE and visualized by Sypro Ruby staining.

(H-J) ITC measurements. **(H)** ZNF4-MIU binding to K48-linked tetraUb **(I)** ZUFSP^{ZNF4-MIU-Cat C360A} binding to K48-linked tetraUb **(J)** ZUFSP^{ZNF4-MIU-Cat C360A} binding to K63-linked tetraUb. K_d and ΔH values of each measurement are indicated.

Figure S6

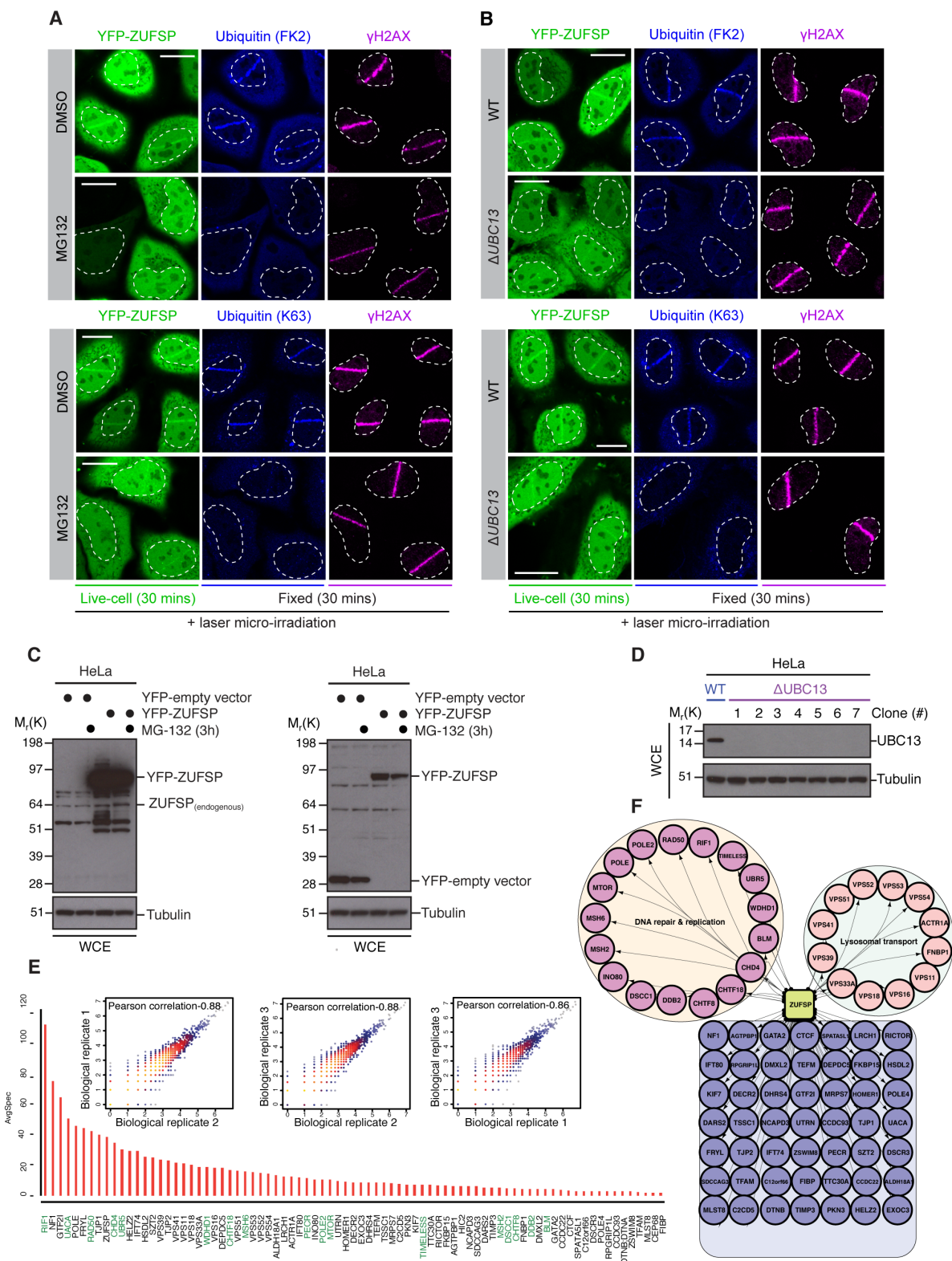


Figure S6 (related to Figure 6).

Analysis of the ZUFSP interactome and the impact of ubiquitin signaling on ZUFSP recruitment to DNA lesions.

(A) HeLa cells were transfected with YFP-ZUFSP, treated with DMSO or MG132 (3h) and then subjected to laser micro-irradiation and imaged at the indicated time. Cells were subsequently fixed and processed for immunostaining with the indicated antibodies. Scale bar, 10 μm .

(B) HeLa wild type (WT) or UBC13-null (ΔUBC13) cells were transfected with YFP-ZUFSP, subjected to laser micro-irradiation and then imaged at the indicated time. Cells were subsequently fixed and processed for immunostaining with the indicated antibodies. Scale bar, 10 μm .

(C) HeLa cells were transfected with either YFP-empty vector or YFP-ZUFSP, treated with DMSO or MG132 (3h), lysed and then analysed by immunoblotting with the indicated antibodies.

(D) HeLa wild type (WT) and multiple ΔUBC13 clones were lysed and analysed by immunoblotting with the indicated antibodies.

(E) SAINT (Significance Analysis of INteractome) analysis of ZUFSP endogenous immunoprecipitation. Pearson correlation of spectral count values between three biological replicates. In the bottom panel histogram presenting the abundance of interacting proteins is shown. DNA repair and replication proteins are highlighted green.

(F) ZUFSP interaction map, representing high confidence interacting proteins obtained from SAINT output filtered with 1% Bayesian false discovery rate (BFDR). Proteins were clustered according to DAVID GOBP enrichment.

Figure S7

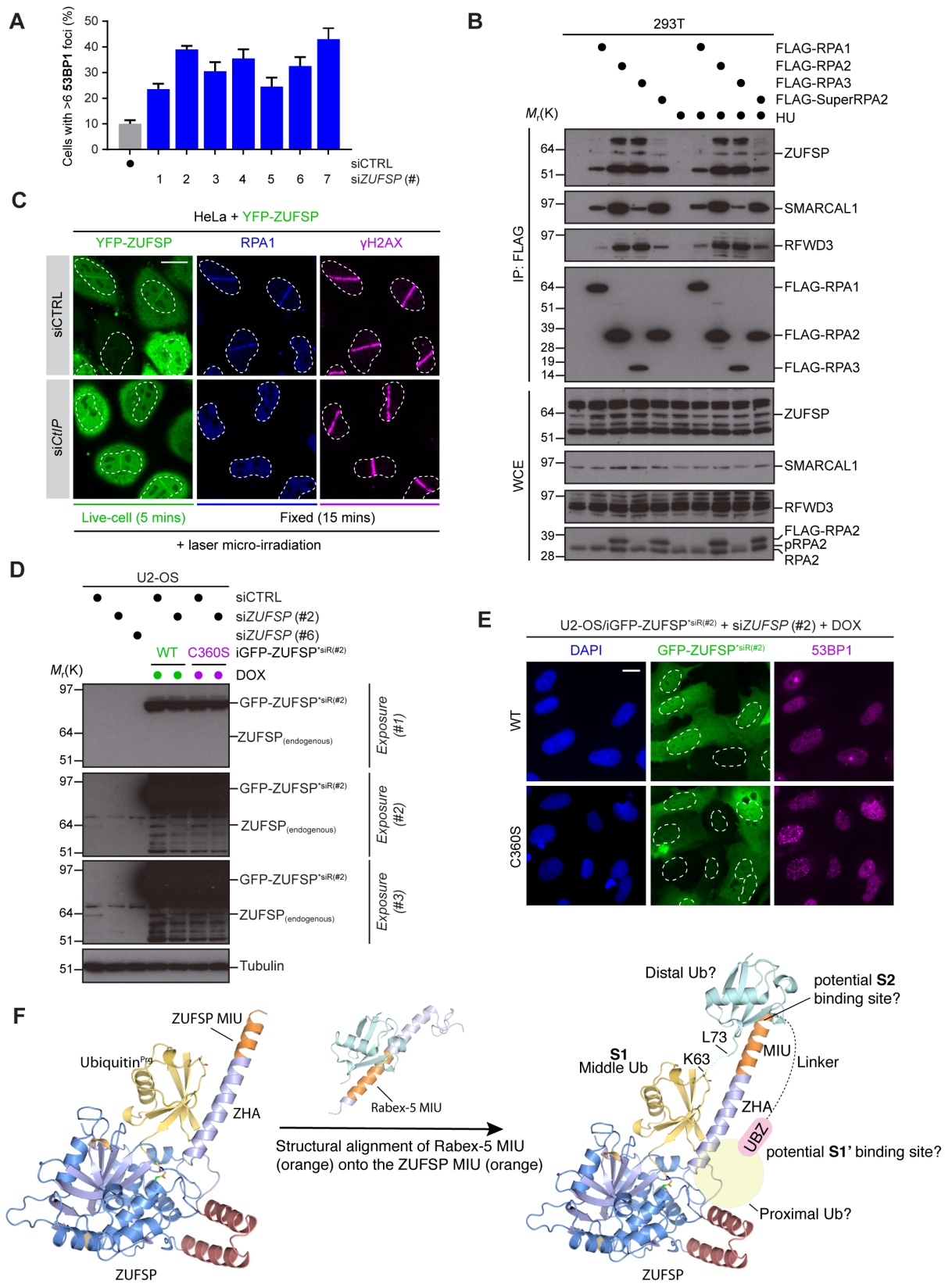


Figure S7 (related to Figure 7).

ZUFSP is functionally involved in DNA repair

(A) U2-OS cells were transfected with control (siCTRL) or ZUFSP (siZUFSP) siRNAs for 72 h. Cells were processed for immunostaining and enumerated for 53BP1 positivity. Data represents mean \pm SEM from two biologically independent experiments using technical duplicates per datapoint.

(B) 293T cells were transfected with FLAG-empty vector, FLAG-RPA1, FLAG-RPA2, FLAG-RPA3 or FLAG-SuperRPA (untagged RPA1, FLAG-RPA2, untagged-RPA3) and treated with hydroxyurea (4 h, 2 mM). Cells were lysed, subjected to FLAG immunoprecipitation and analysed by immunoblotting with the indicated antibodies.

(C) HeLa cells were transfected with control (siCTRL) or CtIP (siCtIP) siRNAs and then further transfected with YFP-ZUFSP. Cells were then subjected to laser micro-irradiation and imaged at the indicated time, fixed and processed for immunostaining with the indicated antibodies. Scale bar, 10 μ m.

(D) U2-OS, U2-OS/iGFP-ZUFSP^{*siR(#2)} wild type (WT) or U2-OS/iGFP-ZUFSP^{*siR(#2)} C360S cells were transfected with either control (siCTRL) or ZUFSP (siZUFSP) siRNAs for 72 h with or without addition of doxycycline. Cells were then lysed and analysed by immunoblotting with the indicated antibodies.

(E) U2-OS/iGFP-ZUFSP^{*siR(#2)} wild type (WT) or U2-OS/iGFP-ZUFSP^{*siR(#2)} C360S cells were transfected with ZUFSP (siZUFSP) siRNA for 72 h with or without addition of doxycycline. Cells were fixed and processed for immunostaining with the indicated antibodies. Enumeration of 53BP1 foci is shown in Figure 7F. Scale bar, 10 μ m.

(F) Model depicting substrate binding and catalysis in ZUFSP. The distal ubiquitin is stabilised by extensive contacts with the ZHA domain and the catalytic core. The MIU motif is partially ordered and does not mediate any interactions with the distal ubiquitin. Ubiquitin binding to MIU was modelled based on the canonical mode of MIU-Ub interaction (PDB ID: 2FIF). Superposition of the RABEX5 MIU-Ub interaction onto the MIU motif of ZUFSP results in ubiquitin binding to the MIU motif in such a way that the C-terminus of the MIU-bound ubiquitin points towards K63 of the ZHA bound distal ubiquitin. This model therefore suggests a K63-linked diubiquitin bound to the long helical arm, i.e. ZHA and MIU. Further, it suggests that the MIU may serve as an S2 binding site. Indeed, mutation of the S2 binding site results

in slightly reduced DUB activity (**Figure S5F**). The polyubiquitin binding UBZ domain (ZNF4) is required for catalytic activity and we suggest that it may form the proximal ubiquitin binding site.

Supplementary Tables (related to Figure 1, 2, 3, 4 and 5).

Table S1

All DNA constructs were made in backbone of the pGEX6P vector for GST-tagged protein unless indicated otherwise.

PROTEIN	DU NUMBER	CONSTRUCT BOUNDRIES
INTEIN constructs		
HA-Ufm1*	47655	1-82
HA-UB*	47186	1-82
HALO-C3-Ub*	55054	1-75
DUBs		
Ufsp1 (Mm)	55016	1-448
OTUD6A**	20889	1-288
ZUFSP HALO-tag constructs		
ZUFSP HALO-MIU	55532	225-267
ZUFSP HALO-ZNF3,4,MIU	24215	145-267
ZUFSP HALO-ZNF4-MIU	55605	186-578
ZUFSP HALO-ZNF3,4	55606	147-220
ZUFSP HALO-ZNF3	55703	147-186
ZUFSP HALO-ZNF4	55689	186-225
ZUFSP HALO-ZNF1,2	55762	1-66
ZUFSP HALO-ZNF1	55764	1-24
ZUFSP HALO-ZNF2	55786	26-66
ZUFSP HALO-ZNF1-4,ZHA,MIU	55787	1-267
ZUFSP HALO-ZNF1-4	55763	1-217
ZUFSP HALO-ZNF4 L200A, I201A	55955	186-225
ZUFSP HALO-ZNF4 N204A, Y205A	55956	186-225
ZUFSP HALO-ZNF4 I207A, L208A	55957	186-225
ZUFSP HALO-ZNF4 Q209A, E210A	55958	186-225
DUB assay constructs		
ZUFSP ^{Cat}	53622	P294-578
ZUFSP ^{ZHA-Cat}	27537	248-578
ZUFSP ^{MIU-Cat}	53621	S231-578

ZUFSP ^{ZNF4-MIU-Cat}	56330	184-578
ZUFSP ^{ZNF3,4-MIU-Cat}	55685	S145-578
ZUFSP ^{ZNF4-MIU-Cat} C360A	55760	184-578
ZUFSP ^{ZNF4-MIU-Cat} C360S	59209	184-578
ZUFSP ^{ZNF4-MIU-Cat} H491A	55797	184-579
ZUFSP ^{ZNF4-MIU-Cat} Y267A	59010	184-579
ZUFSP ^{ZNF4-MIU-Cat} L269A	59011	184-579
ZUFSP ^{ZNF4-MIU-Cat} Q487A	59040	184-579
ZUFSP ^{ZNF4-MIU-Cat} D512A	59064	184-579
ZUFSP ^{ZNF4-MIU-Cat L236A} A237G	59168	184-579
ZUFSP ^{ZNF4-MIU-Cat I207A, L208A}	59189	184-579
ZUFSP ^{MIU-Cat-linker-ZNF4}	55967	250-578-5XGS-186-225

*pTXB1

**pET156P-1

***pMEX3C